

Trainable ISTA for Sparse Signal Recovery

Daisuke Ito*, Satoshi Takabe[†], and Tadashi Wadayama*

*Nagoya Institute of Technology, Gokiso, Nagoya, Aichi, 466-8555, Japan,
d.ito.480@stn.nitech.co.jp, {s_takabe, wadayama}@nitech.ac.jp

[†]RIKEN Center for Advanced Intelligence Project, Nihonbashi, Chuo-ku, Tokyo, 103-0027, Japan,

Abstract—In this paper, we propose a novel sparse signal recovery algorithm called Trainable ISTA (TISTA). The proposed algorithm consists of two estimation units such as a linear estimation unit and a minimum mean squared error (MMSE) estimator-based shrinkage unit. The estimated error variance required in the MMSE shrinkage unit is precisely estimated from a tentative estimate of the original signal. The remarkable feature of the proposed scheme is that TISTA includes adjustable variables controlling a step size and the error variance for the MMSE shrinkage. The variables are adjusted by standard deep learning techniques. The number of trainable variables of TISTA is equal to the number of iteration rounds and it is much smaller than that of known learnable sparse signal recovery algorithms. This feature leads to highly stable and fast training processes of TISTA. Computer experiments show that TISTA is applicable to various classes of sensing matrices such as Gaussian matrices, binary matrices and matrices with large condition numbers. Numerical results also demonstrate that TISTA shows significantly faster convergence than those of AMP and LISTA in many cases.

I. INTRODUCTION

The basic problem setup for *compressed sensing* [1], [2] is as follows. A real vector $x \in \mathbb{R}^N$ represents the source sparse signal. It is assumed that we cannot directly observe x but we observe $y = Ax + w$ where $A \in \mathbb{R}^{M \times N}$ ($N \geq M$) is a sensing matrix and $w \in \mathbb{R}^M$ is a Gaussian noise vector. Our goal is to estimate x from y as correct as possible.

For a number of sparse reconstruction algorithms [3], Lasso formulation [4] is fairly common for solving the sparse signal recovery problems. In Lasso formulation, the original problem is recast as a convex optimization problem for minimizing $\frac{1}{2}\|y - Ax\|_2^2 + \lambda\|x\|_1$. The regularization term $\lambda\|x\|_1$ promotes sparseness of a reconstruction vector where λ is the regularization constant. In order to solve the Lasso problem efficiently, a number of algorithms have been developed [5]. Iterative Shrinkage Thresholding Algorithm (ISTA) [6], [7] is one of the most known algorithms for solving the Lasso problem. ISTA is an iterative algorithm comprising of two processes, i.e., a linear estimation process and a shrinkage process based on a soft thresholding function. ISTA can be seen as a proximal gradient descent algorithm [8] and it can be directly derived from Lasso formulation.

Approximate Message Passing (AMP) [9], [10] which is a variant of approximate belief propagation, shows much faster convergence than that of ISTA in general. The remarkable feature of AMP is that its asymptotic behavior is completely described by the state evolution equations [11]. AMP is derived based on the assumption that the sensing matrices

consist of i.i.d. Gaussian distributed components. Recently, Ma and Ping proposed Orthogonal AMP (OAMP) [13] that can handle various classes of sensing matrices including unitary invariant matrices. Rangan et al. proposed VAMP [14] for right-rotationally invariant matrices and provided a theoretical justification for its state evolution. Independently, Takeuchi [15] also gave a rigorous analysis for a sparse recovery algorithm for unitary invariant measurements based on the expectation propagation framework.

The advent of recent powerful neural networks (NN) triggered explosive spread of research activities and applications on deep neural networks (DNN) [16]. The DNN have found a number of practical applications such as image recognition [17], [18], speech recognition [19] and robotics because of their outstanding performance compared with the traditional methods. The advancement of DNN are also giving impact on design of algorithms for communications and signal processing [20], [21]. By unfolding an iterative process of a sparse signal recovery algorithm, we can obtain a *signal-flow graph*. The signal-flow graph includes trainable variables that can be tuned with a supervised leaning method, i.e., standard deep learning techniques such as stochastic gradient descent algorithms based on the back propagation and mini-batches can be used to adjust the trainable parameters. Gregor and LeCun presented Learned ISTA (LISTA) [22] that employs learnable threshold variables for a shrinkage function. It is shown that LISTA yields recovery performance superior to that of the original ISTA. Borgerding et al. also presented variants of AMP and VAMP with learnable capability [23] [24].

The goal of this work is to propose a simple sparse recovery algorithm based on deep learning techniques. The proposed algorithm, called *Trainable ISTA (TISTA)*, borrows the basic structure from ISTA, and an estimator of the squared error between true signals and tentative estimations, i.e., the *error variance estimator*, from OAMP. Thus, TISTA comprises of the three parts: a linear estimator, an minimum mean squared error (MMSE) estimator-based shrinkage function, and the error variance estimator. The linear estimator of TISTA includes trainable variables that can be adjusted via deep learning techniques.

II. BRIEF REVIEW OF KNOWN RECOVERY ALGORITHMS

As preparation for describing the details of the proposed algorithm, several known sparse recovery algorithms are briefly reviewed in this section. In the following, the observation vector is assumed to be $y = Ax + w$ where $A \in \mathbb{R}^{M \times N}$ ($N \geq M$)

and $x \in \mathbb{R}^N$. Each entry of additive noise vector $w \in \mathbb{R}^M$ obeys zero mean Gaussian distribution with variance σ^2 .

A. ISTA

ISTA is a well-known sparse recovery algorithm [6] defined by the following simple recursion: $r_t = s_t + \beta A^T(y - As_t)$, $s_{t+1} = \eta(r_t; \tau)$, where β represents a step size and η is the soft thresholding function defined by $\eta(r; \tau) = \text{sign}(r) \max\{|r| - \tau, 0\}$. The parameter $\tau (> 0)$ indicates the threshold value. After T -iterations, the estimate $\hat{x} = s_T$ of the original sparse signal x is obtained. The initial value is assumed to be $s_0 = 0$. In order to have convergence, the step parameter should be carefully determined [6]. Several accelerated methods for ISTA using a momentum term have been proposed [25], [26]. Since the proximal operator of L_1 -regularization term $\|x\|_1$ is the soft thresholding function, ISTA can be seen as a proximal gradient descent algorithm [3].

B. AMP

AMP [10] is defined by the following recursion:

$$r_t = y - As_t + b_t r_{t-1}, \quad (1)$$

$$s_{t+1} = \eta(s_t + A^T r_t; \tau_t), \quad (2)$$

$$b_t = \frac{1}{M} \|s_t\|_0, \quad \tau_t = \frac{\theta}{\sqrt{M}} \|r_t\|_2 \quad (3)$$

and it provides the final estimate $\hat{x} = s_T$. It is assumed that each entry of the sensing matrix A is generated according to the Gaussian distribution $\mathcal{N}(0, 1/M)$, i.e., Gaussian distribution with mean zero and variance $1/M$. The recursive formula of AMP seem similar to these of ISTA at a glance but there are several critical differences. Due to the *Onsager correction term* $b_t r_{t-1}$ in (1), the output of the linear estimator becomes statistically decoupled and an error between each output signal from the linear estimator and the true signal behaves as a white Gaussian random variable in large system limit. This enable us to use a scalar recursion called the *state evolution* to track the evolution of the error variances. Another difference between ISTA and AMP is the estimator of τ_t in (3), which is used as the threshold value for the shrinkage function (2). In [10], it is reported that AMP shows much faster convergence than that of ISTA if the sensing matrix satisfies the above condition. However, it is known that AMP cannot provide excellent recovery performance for sensing matrices violating the above condition such as non-Gaussian sensing matrices, Gaussian matrices with large variance, Gaussian matrices with non-zero mean, and matrices with large condition numbers [12].

C. OAMP

OAMP [13] is defined by the following recursive formula:

$$r_t = s_t + W_t(y - As_t), \quad (4)$$

$$s_{t+1} = \eta_{\text{df}}(r_t; \tau_t), \quad (5)$$

$$v_t^2 = \max \left\{ \frac{\|y - As_t\|_2^2 - M\sigma^2}{\text{trace}(A^T A)}, \epsilon \right\}, \quad (6)$$

$$\tau_t^2 = \frac{1}{N} \text{trace}(B_t B_t^T) v_t^2 + \frac{1}{N} \text{trace}(W_t W_t^T) \sigma^2, \quad (7)$$

$$B_t = I - W_t A, \quad (8)$$

for $t = 0, 1, 2, \dots, T-1$. To be precise, the estimator equations on v_t^2 (6) and τ_t^2 (7) (presented also in [27]) are not part of OAMP (for example, we can use the state evolution to provide v_t^2 and τ_t^2) but these estimators were adopted numerical evaluation in [13]. The matrix W_t in linear estimator (4) can be chosen from the transpose of A , the pseudo inverse of A and the LMMSE matrix. The nonlinear estimation unit (5) consists of a *divergence free function* η_{df} that replaces the Onsager correction term. It is proved in [13] that the estimation errors at the linear estimator (4) and non-linear estimator (5) are statistically orthogonal if a sensing matrix is i.i.d. Gaussian or unitary invariant. This fact provides a justification for the state evolution of OAMP.

III. DETAILS OF TISTA

This section describes the details of TISTA and its training process.

A. MMSE estimators for additive Gaussian noise channel

Let X be a real-valued random variable with probability density function (PDF) $P_X(\cdot)$. We assume an additive Gaussian noise channel defined by $Y = X + N$, where Y represents a real-valued random variable as well. The random variable N is a Gaussian random variable with mean 0 and variance σ^2 . Consider the situation where a receiver can observe Y and wish to estimate the value of X .

The MMSE estimator $\eta_{\text{MMSE}}(y)$ is defined $\eta_{\text{MMSE}}(y) = \mathbb{E}[X|y]$ where $\mathbb{E}[X|y]$ is the conditional expectation given by

$$\mathbb{E}[X|y] = \int_{-\infty}^{\infty} x P(x|y) dx. \quad (9)$$

The posterior PDF $P(x|y)$ is given by Bayes Theorem:

$$P_{X|Y}(x|y) = \frac{P_X(x) P_{Y|X}(y|x)}{P_Y(y)}, \quad (10)$$

where the conditional PDF is Gaussian:

$$P_{Y|X}(y|x) = \frac{1}{\sqrt{2\pi}\sigma^2} \exp\left(-\frac{(y-x)^2}{2\sigma^2}\right). \quad (11)$$

In the case of the Bernoulli-Gaussian prior, $P_X(x)$ is given by

$$P_X(x) = (1-p)\delta(x) + \frac{p}{\sqrt{2\pi}\alpha^2} \exp\left(-\frac{x^2}{2\alpha^2}\right), \quad (12)$$

where p represents the probability such that a non-zero element occurs. The function $\delta(\cdot)$ is the Dirac's delta function. In this case, a non-zero element follows the Gaussian PDF with mean zero and variance α^2 . The MMSE estimator for the Bernoulli-Gaussian prior can be easily derived [29] by using Stein's formula:

$$\eta_{\text{MMSE}}(y; \sigma^2) = y + \sigma^2 \frac{d}{dy} \ln P_Y(y) \quad (13)$$

and we have

$$\eta_{\text{MMSE}}(y; \sigma^2) = \left(\frac{y\alpha^2}{\xi} \right) \frac{pF(y; \xi)}{(1-p)F(y; \sigma^2) + pF(y; \xi)}, \quad (14)$$

where $\xi = \alpha^2 + \sigma^2$ and

$$F(z; v) = \frac{1}{\sqrt{2\pi v}} \exp\left(\frac{-z^2}{2v}\right). \quad (15)$$

These MMSE estimators are going to be used as a building block of TISTA to be presented in the next subsection.

B. Recursive formula for TISTA

We assume that the sensing matrix $A \in \mathbb{R}^{M \times N}$ is a full rank matrix. The recursive formula of TISTA are summarized as follows:

$$r_t = s_t + \gamma_t W(y - As_t), \quad (16)$$

$$s_{t+1} = \eta_{MMSE}(r_t; \tau_t^2), \quad (17)$$

$$v_t^2 = \max\left\{\frac{\|y - As_t\|_2^2 - M\sigma^2}{\text{trace}(A^T A)}, \epsilon\right\}, \quad (18)$$

$$\begin{aligned} \tau_t^2 &= \frac{v_t^2}{N}(N - 2\gamma_t \text{trace}(Z) + \gamma_t^2 \text{trace}(ZZ^T)) \\ &+ \frac{\gamma_t^2 \sigma^2}{N} \text{trace}(WW^T), \end{aligned} \quad (19)$$

where the matrix $W = A^T(AA^T)^{-1}$ is the pseudo inverse matrix¹ of the sensing matrix A , and $Z = WA$. The initial condition is $s_0 = 0$ and the final estimate is given by $\hat{x} = s_T$. The scalar variables $\gamma_t \in \mathbb{R}(t = 0, 1, \dots, T-1)$ are learnable variables that are tuned in a training process. The number of learnable variables is thus T that is much smaller than that of LISTA [22] and LAMP [23].

An appropriate MMSE shrinkage (17) is chosen according to the prior distribution of the original signal x . Note that the MMSE shrinkage is also employed in [23]. The real constant ϵ is a sufficiently small value, e.g., $\epsilon = 10^{-9}$. The max operator in (18) is employed to prevent the estimate of the variance being non-positive. The learnable variables γ_t in (16) provide appropriate step sizes and control for the variance of the MMSE shrinkage.

The true error variances $\bar{\tau}_t^2$ and \bar{v}_t^2 are defined by

$$\bar{\tau}_t^2 = \mathbb{E}[\|r_t - x\|_2^2]/N, \quad \bar{v}_t^2 = \mathbb{E}[\|s_t - x\|_2^2]/N. \quad (20)$$

These error variances should be estimated as correct as possible in a sparse recovery process because the MMSE shrinkage (17) requires to know $\bar{\tau}_t^2$. As in the case of OAMP [13], we make the following assumptions on the residual errors in order to derive an error variance estimator.

The first assumption is that $r_t - x$ consists of i.i.d. zero mean Gaussian entries. Due to this assumption, each entry of the output from the linear estimator (16) can be seen as an observation obtained from a virtual additive Gaussian noise channel with the noise variance $\bar{\tau}^2$. This justifies the use of the shrinkage function based on the MMSE estimator (17) with $\bar{\tau}^2$. Another assumption is that $s_t - x$ consists of zero mean i.i.d. entries and satisfies $\mathbb{E}[(s_t - x)^T A^T w] = \mathbb{E}[(s_t - x)^T W w] = 0$ for any t .

¹If $N < M$, we let $W = (A^T A)^{-1} A^T$.

The error variance estimator for \bar{v}_t^2 (18) is the same as that of OAMP [13] and its justification comes from the following proposition.

Proposition 1: If each entry of $s_t - x$ is i.i.d. with mean 0 and $\mathbb{E}[(s_t - x)^T A^T w] = 0$ is satisfied, then

$$\bar{v}_t^2 = \frac{\mathbb{E}[\|y - As_t\|_2^2] - M\sigma^2}{\text{trace}(A^T A)} \quad (21)$$

holds.

The justification of the error variance estimator (19) for $\bar{\tau}_t^2$ is also provided by the following proposition.

Proposition 2: If each entry of $s_t - x$ is i.i.d. with mean 0 and $\mathbb{E}[(s_t - x)^T W w] = 0$ is satisfied, then

$$\begin{aligned} \bar{\tau}_t^2 &= \frac{\bar{v}_t^2}{N}(N - 2\gamma_t \text{trace}(Z) + \gamma_t^2 \text{trace}(ZZ^T)) \\ &+ \frac{\gamma_t^2 \sigma^2}{N} \text{trace}(WW^T) \end{aligned} \quad (22)$$

holds.

(Proof) The residual error $r_t - x$ can be rewritten as

$$\begin{aligned} r_t - x &= s_t + \gamma_t W(y - As_t) - x \\ &= s_t + \gamma_t W(Ax + w) - \gamma_t WAs_t - x \\ &= (I - \gamma_t Z)(s_t - x) + \gamma_t Ww. \end{aligned}$$

From the definition $\bar{\tau}_t^2$, we have

$$\begin{aligned} \bar{\tau}_t^2 &= \frac{1}{N} \mathbb{E}[\|(I - \gamma_t Z)(s_t - x) + \gamma_t Ww\|_2^2] \\ &= \frac{1}{N} \mathbb{E}[(s_t - x)^T (I - \gamma_t Z)(I - \gamma_t Z)^T (s_t - x)] \\ &+ \frac{\gamma_t^2}{N} \mathbb{E}[w^T W^T W w] + \frac{2\gamma_t}{N} \mathbb{E}[(s_t - x)^T (I - \gamma_t Z)^T W w] \\ &= \frac{1}{N} \text{trace}((I - \gamma_t Z)(I - \gamma_t Z)^T) \bar{v}_t^2 \\ &+ \frac{\gamma_t^2}{N} \text{trace}(WW^T) \sigma^2 + \frac{2(\gamma_t - \gamma_t^2)}{N} \mathbb{E}[(s_t - x)^T W w]. \end{aligned}$$

The last term vanishes due to the assumption $\mathbb{E}[(s_t - x)^T W w] = 0$ and the first term can be rewritten as

$$\begin{aligned} &\text{trace}((I - \gamma_t WA)(I - \gamma_t WA)^T) \\ &= \sum_{i,j:i \neq j} (\gamma_t Z_{i,j})^2 + \sum_i (1 - \gamma_t Z_{i,i})^2 \\ &= \gamma_t^2 \sum_{i,j:i \neq j} Z_{i,j}^2 + \sum_i (1 - 2\gamma_t Z_{i,i} + \gamma_t^2 Z_{i,i}^2) \\ &= N - 2\gamma_t \text{trace}(Z) + \gamma_t^2 \text{trace}(ZZ^T). \end{aligned} \quad (23)$$

The claim of the proposition is now obtained. (QED)

These error variance estimators (18) and (19) play a crucial role to give appropriate variance estimates required for the MMSE shrinkage. Since the validity of these assumptions on the residual errors cannot be proved, it will be experimentally confirmed in the next section. It should be also remarked that the TISTA recursive formula does not include neither an Onsager correction term nor a divergence free function. Thus, we cannot expect stochastic orthogonality guaranteed in OAMP in a process of TISTA. This means that the state evolution cannot be applied to analyze the asymptotic performance of TISTA.

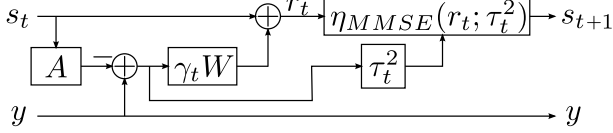


Fig. 1. The t -th iteration of the TISTA with learnable variable γ_t

C. Time complexity of TISTA

For treating a large scale problem, a sparse recovery algorithm should require low computational complexity for each iteration. The time complexity required for evaluating the recursive formula of TISTA per iteration is $O(N^2)$, which is the same time complexity as those of ISTA and AMP, which means that TISTA has sufficient scalability for large problems. The evaluation of the matrix-vector products, As_t and $W(y - As_t)$ need $O(N^2)$ -time that are dominant in an iteration. Although the evaluations of the scalar constants $\text{trace}(A^T A)$, $\text{trace}(WW^T)$, and $\text{trace}(ZZ^T)$ and computation of the pseudo inverse of A require $O(N^3)$ -time, they can be pre-computed only once in advance.

D. Incremental training for TISTA

In order to achieve reasonable recovery performance, the trainable variables $\gamma_t (t = 0, 1, \dots, T-1)$ should be appropriately adjusted. By unfolding the recursive formula of TISTA, we immediately have a signal-flow graph which is similar to a multi-layer feedforward neural network. Figure 1 depicts a unit of the signal-flow graph corresponding to t -th iteration of TISTA and we can stack the units to compose a whole signal-flow graph. We here follow a standard recipe of deep learning techniques, namely we apply mini-batch training with a stochastic gradient descent algorithm to the signal-flow graph of TISTA. From several experiments, we found that the following *incremental training* is considerably effective to learn appropriate values providing superior performance.

The training data consists of a number of randomly generated pairs (x, y) where $y = Ax + w$. The sample x follows the prior distribution $P_X(x)$ and w is an i.i.d. Gaussian random vector. The whole training data is divided into mini-batches to be used in a stochastic gradient descent algorithm such as SGD, RMSprop or Adam.

In the t -th round of the incremental training (we call it a *generation*), an optimizer tries to minimize $\mathbb{E}[\|s_t - x\|_2^2]$ by tuning $\gamma_0, \gamma_1, \dots, \gamma_{t-1}$. The number of mini-batches used in t -th generation is denoted by D (epochs). After processing D epochs, the target of the optimizer is changed to $\mathbb{E}[\|s_{t+1} - x\|_2^2]$. Namely, after training the first to t -th layers, a new $t+1$ layer is appended to the network and the whole network is trained again for D epochs. Although the objective function is changed, the values of the variables $\gamma_0, \dots, \gamma_{t-1}$ of the previous generation is taken over as the initial values in the optimization process for the new generation. In summary, the incremental training updates the variables γ_t in a sequential manner from the first layer to the last layer.

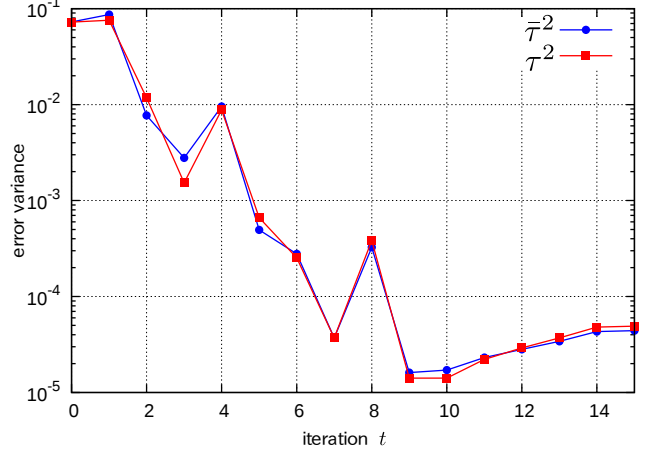


Fig. 2. Comparison between the estimate $\hat{\tau}^2$ and the true error variance τ^2 ; $A \sim \mathcal{N}(0, 1/M)$, SNR = 40 dB. The optimized γ_t in this case are given by $\gamma_0 = 1.67, \gamma_1 = 4.42, \gamma_2 = 1.41, \gamma_3 = 1.35, \gamma_4 = 5.66, \gamma_5 = 1.51, \gamma_6 = 2.83, \gamma_7 = 1.38, \gamma_8 = 5.84, \gamma_9 = 0.92, \gamma_{10} = 1.13, \gamma_{11} = 1.49, \gamma_{12} = 1.70, \gamma_{13} = 1.91, \gamma_{14} = 2.18, \gamma_{15} = 2.21$.

IV. PERFORMANCE EVALUATION

A. Details of experiments

The basic conditions for computer experiments are summarized as follows. Each component of the sparse signal x is assumed to be a realization of i.i.d. random variable following the Bernoulli-Gaussian PDF (12) with $p = 0.1, \alpha^2 = 1$. We thus use the MMSE estimator (17) for the Bernoulli-Gaussian prior. Each component of the noise vector w follows the zero mean Gaussian PDF with variance σ^2 . The signal to noise ratio (SNR) of the system is defined as $\text{SNR} = \mathbb{E}[\|Ax\|_2^2] / \mathbb{E}[\|w\|_2^2]$. The dimension of the sensing matrices are set to be $N = 500, M = 250$. The size of the mini-batch is set to 1000, and $D = 200$ epochs are allocated for each generation. We used Adam optimizer with the initial value 4.0×10^{-2} in the training phase. The experiment system was implemented based on TensorFlow [28]. For comparison purpose, we will include the NMSE performances of AMP and LISTA in the following subsections. The hyper parameter θ used in AMP is set to $\theta = 1.14$. We used an implementation of LISTA by Borgerding [30].

B. IID Gaussian matrix

This subsection describes the case where $A \sim \mathcal{N}(0, 1/M)$, i.e., each component of the sensing matrix A obeys zero mean Gaussian distribution with variance $1/M$. Note that AMP is designed for this matrix ensemble.

Figure 2 shows a comparison between the estimate τ^2 by (19) and the empirically estimated values of the true error variance $\hat{\tau}^2$. We can observe that the estimator τ^2 provides accurate estimations and it justifies the use of (18) and (19) and our assumptions on the residual errors. The caption of Fig. 2 includes a set of the optimized γ_t .

Figure 3 presents the average normalized MSE (NMSE) of TISTA, LISTA and AMP as functions of iteration when

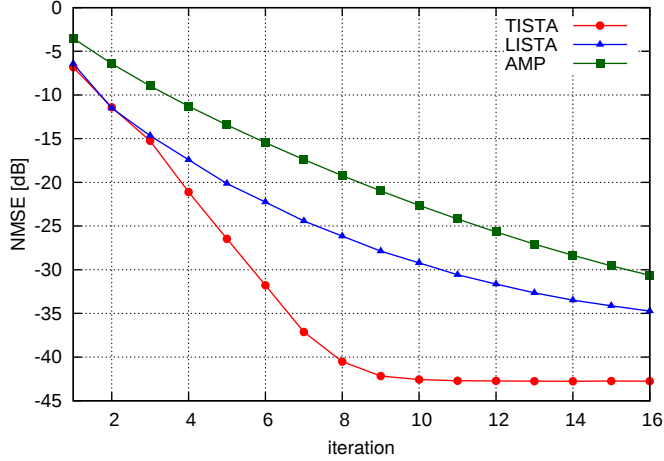


Fig. 3. NMSE of TISTA, LISTA and AMP; $A_{i,j} \sim \mathcal{N}(0, 1/M)$, SNR = 40dB. The condition $A_{i,j} \sim \mathcal{N}(0, 1/M)$ is required for AMP to converge.

SNR = 40dB. The NMSE is defined by $10 \log_{10} \{ \|s_{t+1} - x\|_2^2 / \|x\|_2^2 \}$ (dB). From Fig. 3, we can observe that TISTA provides the steepest NMSE curve than those of AMP and LISTA at the first 16 rounds. For example, AMP and LISTA require 16 and 10 rounds to achieve NMSE = -30dB, respectively, but TISTA needs only 6 rounds. It can be seen that the NMSE curve of TISTA saturates around -43dB at which TISTA converges. This means that TISTA shows significantly faster convergence than that of AMP and LISTA in this setting. Compared with the experimental results under the same condition shown in [24], the NMSE values of TISTA is almost comparable to those of LAMP [23]. CPU time required for training a 7-layers TISTA graph was around 6 minutes by using a PC with GPU NVIDIA GeForce GTX 1080. A large Gaussian matrix with the size $N = 5000, M = 2500$ required around 7 hours for training. It was observed that the NMSE curve of $N = 5000$ is quite similar to that of $N = 500$.

In the next experiment, we made change on the variance of sensing matrices to a larger number, i.e., each element in A follows $\mathcal{N}(0, 1)$. Figure 4 shows the NMSE curves of TISTA and LISTA. It should be noted that, under this condition, AMP does not perform well, i.e., it cannot converge at all, because the setting does not fit the required condition ($A_{i,j} \sim \mathcal{N}(0, 1/M)$) for achieving the guaranteed performance and the convergence of AMP. As we can see from Fig. 4, TISTA behaves soundly and shows faster convergence than that of LISTA. This result suggests that TISTA is appreciably robust against the change of the variance.

C. Binary matrix

In this subsection, we will discuss the case where sensing matrices are binary, i.e., $A \in \{\pm 1\}^{M \times N}$. Each entry of A is selected uniformly at random on $\{\pm 1\}$. This situation is closely related to multiuser detection in Coded Division Multiple Access (CDMA) [9]. Figure 5 shows the NMSE curves of TISTA and LISTA as a function of iteration. It can

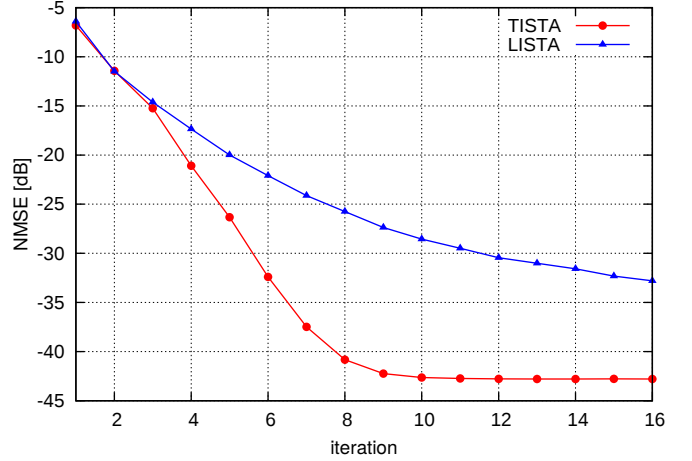


Fig. 4. NMSE of TISTA and LISTA; $A_{i,j} \sim \mathcal{N}(0, 1)$, SNR = 40dB. In this case, AMP cannot converge because the variance of the matrix components are too large.

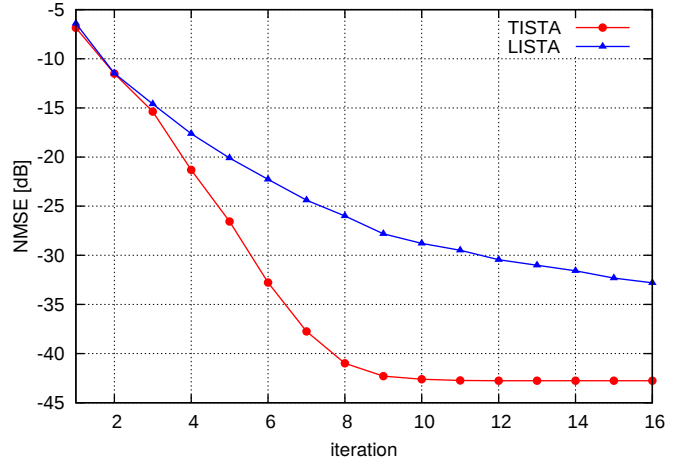


Fig. 5. NMSE of TISTA and LISTA; $A_{i,j}$ takes a value in $\{\pm 1\}$ uniformly at random. SNR = 40dB. AMP is not applicable to this case.

be seen that the NMSE curves of TISTA almost coincide with those of the Gaussian sensing matrices. This result can be regarded as an evidence for the robustness of TISTA for non-Gaussian sensing matrices.

D. Sensing matrices with large condition number

The condition number κ of a matrix is defined as the ratio of the largest and the smallest singular values, i.e., $\kappa = s_1/s_M$ where $s_1 \geq s_2 \geq \dots \geq s_M$ are the singular values of the matrix. It is known that regression problems regarding a matrix with a large condition number are difficult to solve in an accurate manner. In this subsection, we access the performance of TISTA for sensing matrices with a large condition number. Figure 6 presents NMSE of TISTA and AMP when SNR = 60dB. AMP can converge up to $\kappa = 4$ but it diverges when $\kappa > 4$. TISTA shows similar performance of AMP with $\kappa = 4$ even when $\kappa = 1000$. This result is a strong evidence

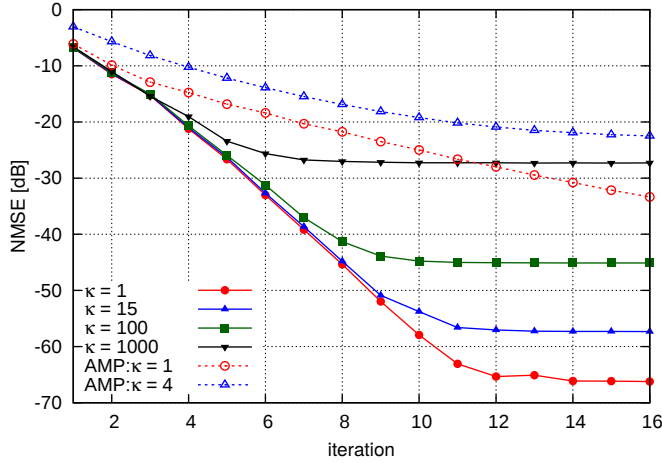


Fig. 6. NMSE of TISTA and AMP; κ represents the condition number. SNR = 60dB. The singular values are selected so that s_i/s_{i-1} becomes a constant. The sensing matrix A is normalized as $\|A\|_F^2 = N$.

that TISTA has a potential to achieve excellent NMSE even for a sensing matrix with a large condition number.

V. CONCLUDING SUMMARY

The crucial feature of TISTA is that it includes adjustable variables which can be tuned by standard deep learning techniques. The number of trainable variables of TISTA is equal to the number of iterative rounds and it is much smaller than those of the known learnable sparse signal recovery algorithms [22]–[24]. This feature leads to highly stable and fast training processes of TISTA. Computer experiments indicate that TISTA is applicable to various classes of sensing matrices such as Gaussian matrices, binary matrices and matrices with large condition numbers. Furthermore, numerical results demonstrate that TISTA shows significantly faster convergence than those of AMP and LISTA in many cases. By replacing the MMSE shrinkage, we can expect that TISTA is also applicable to non-sparse signal recovery problems such as detection of BPSK signals in overloaded MIMO systems.

ACKNOWLEDGEMENT

This work is supported by JSPS Grant-in-Aid for Scientific Research (B) Grant Number 16H02878 (TW) and Grant-in-Aid for Young Scientists (Start-up) Grant Number 17H06758 (ST). The last author is grateful to Keigo Takeuchi for an inspiring seminar talk.

REFERENCES

- [1] D. L. Donoho, "Compressed sensing," *IEEE Trans. Inf. Theory*, vol. 52, no. 4, pp. 1289–1306, Apr. 2006.
- [2] E. J. Candes and T. Tao, "Near-optimal signal recovery from random projections: Universal encoding strategies?" *IEEE Trans. Inf. Theory*, vol. 52, no. 12, pp. 5406–5425, Dec. 2006.
- [3] Z. Zhang, Y. Xu, J. Yang, X. Li, and D. Zhang, "A Survey of Sparse Representation: Algorithms and Applications," *IEEE Access*, vol. 3, pp. 490–530, 2015.
- [4] R. Tibshirani, "Regression shrinkage and selection via the lasso," *J. Royal Stat. Society, Series B*, vol. 58, pp. 267–288, 1996.
- [5] B. Efron, T. Hastie, I. Johnstone, and R. Tibshirani, "Least Angle Regression," *Ann. Stat.*, vol. 32, no. 2, pp. 407–499, Apr. 2004.
- [6] A. Chambolle, R. A. DeVore, N. Lee, and B. J. Lucier, "Nonlinear wavelet image processing: variational problems, compression, and noise removal through wavelet shrinkage," *IEEE Trans. Image Process.*, vol. 7, no. 3, pp. 319–335, Mar. 1998.
- [7] I. Daubechies, M. Defrise, and C. De Mol, "An iterative thresholding algorithm for linear inverse problems with a sparsity constraint," *Comm. Pure and Appl. Math.*, col. 57, no. 11, pp. 1413–1457, Nov. 2004.
- [8] N. Parikh and S. Boyd, "Proximal Algorithms," *Foundations and Trends in Optimization*, vol. 1, no. 3, pp. 127–239, 2014.
- [9] Y. Kabashima, "A CDMA multiuser detection algorithm on the basis of belief propagation," *J. Phys. A: Math. Gen.*, vol. 36 11111–11121, Oct. 2003.
- [10] D. L. Donoho, A. Maleki, and A. Montanari, "Message-passing algorithms for compressed sensing," *Proceedings of the National Academy of Sciences*, vol. 106, no. 45, pp. 18914–18919, Nov. 2009.
- [11] D. L. Donoho, A. Maleki, and A. Montanari, "Message passing algorithms for compressed sensing: I. Motivation and construction," *IEEE Information Theory Workshop 2010, ITW 2010*, pp. 1–5, 2010.
- [12] F. Caltagirone, L. Zdeborova, and F. Krzakala, "On convergence of approximate message passing," *2014 IEEE Int. Symp. Inf. Theory*, Jun. 2014, pp. 1812–1816.
- [13] J. Ma and L. Ping, "Orthogonal AMP," *IEEE Access*, vol. 5, pp. 2020–2033, 2017.
- [14] S. Rangan, P. Schniter, and A. K. Fletcher, "Vector approximate message passing," *2017 IEEE Int. Symp. Inf. Theory*, Jun. 2017, vol. 65, no. 17, pp. 1588–1592.
- [15] K. Takeuchi, "Rigorous dynamics of expectation-propagation-based signal recovery from unitarily invariant measurements," *2017 IEEE Int. Symp. Inf. Theory*, Jun. 2017, pp. 501–505.
- [16] K. Fukushima, "Neocognitron: A self-organizing neural network model for a mechanism of pattern recognition unaffected by shift in position," *Bio. Cybern.*, vol. 36, no. 4, pp. 193–202, 1980.
- [17] G. E. Hinton, R. R. Salakhutdinov, "Reducing the Dimensionality of Data with Neural Networks," *Science*, vol. 313, no. 5786, pp. 504–507, Jun. 2006.
- [18] A. Krizhevsky, I. Sutskever, G. E. Hinton, "Imagenet classification with deep convolutional neural networks," *Advances in Neural Inf. Proc. Sys.* 2012, pp. 1097–1105, 2012.
- [19] G. Hinton et al., "Deep Neural Networks for Acoustic Modeling in Speech Recognition: The Shared Views of Four Research Groups," *IEEE Signal Processing Magazine*, vol. 29, no. 6, pp. 82–97, Nov. 2012.
- [20] B. Aazhang, B. P. Paris and G. C. Orsak, "Neural networks for multiuser detection in code-division multiple-access communications," *IEEE Trans. Comm.*, vol. 40, no. 7, pp. 1212–1222, Jul. 1992.
- [21] E. Nachmani, Y. Be'ery and D. Burshtein, "Learning to decode linear codes using deep learning," *2016 54th Annual Allerton Conf. Comm., Control, and Computing*, 2016, pp. 341–346.
- [22] K. Gregor, and Y. LeCun, "Learning fast approximations of sparse coding," *Proc. 27th Int. Conf. Machine Learning*, pp. 399–406, 2010.
- [23] M. Borgerding and P. Schniter, "Onsager-corrected deep learning for sparse linear inverse problems," *2016 IEEE Global Conf. Signal and Inf. Proc. (GlobalSIP)*, Washington, DC, Dec. 2016, pp. 227–231.
- [24] M. Borgerding, P. Schniter, and S. Rangan, "AMP-Inspired Deep Networks for Sparse Linear Inverse Problems," *arXiv:1612.01183v2* (2017).
- [25] A. Beck, and M. Teboulle, "A fast iterative shrinkage-thresholding algorithm for linear inverse problems," *SIAM J Imaging Sciences*, vol. 2, no. 1, pp. 183–202, 2009.
- [26] J. M. Bioucas-Dias and M. A. T. Figueiredo, "A New TwIST: Two-Step Iterative Shrinkage/Thresholding Algorithms for Image Restoration," *IEEE Trans. Image Proc.*, vol. 16, no. 12, pp. 2992–3004, Dec. 2007.
- [27] J. Vila and P. Schniter, "Expectation-maximization gaussian-mixture approximate message passing," *IEEE Trans. Signal Proc.*, vol. 61, no. 19, pp. 4658–4672, 2013.
- [28] "TensorFlow: Large-scale machine learning on heterogeneous systems," <http://tensorflow.org/> 2015. Software available from tensorflow.org.
- [29] Rémi Gribonval "Should penalized least squares regression be interpreted as Maximum A Posteriori estimation?," *IEEE Transactions on Signal Processing*, vol.59, no.5, pp. 2405–2410, May. 2011.
- [30] https://github.com/mborgerding/onsager_deep_learning/blob/master/README.md